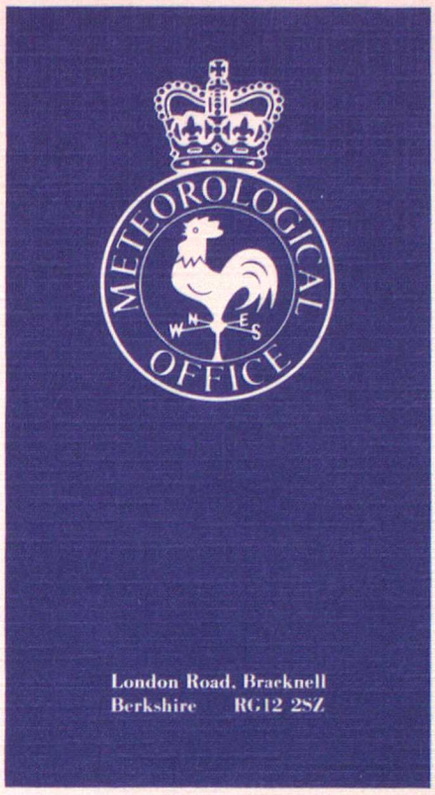

LONDON, METEOROLOGICAL OFFICE.

Met.O.11 Technical Note No.220.

Fine-mesh data assimilation scheme. By BELL,R.S.

London,Met.Off.,Met.O.11 Tech.Note No.220, 1985,30cm.Pp.18,19 pls.8 Refs.

An unofficial document - restriction on first page to be observed.

KW

MET O 11 TECHNICAL NOTE NO 220

The Fine-mesh Data Assimilation Scheme

by R. S. Bell

December 1985

Met O 11
Meteorological Office
London Road
Bracknell
Berkshire

1. Introduction

Fine-mesh limited area forecast models have been an important tool to the forecaster for more than a decade now, but for much of that period little attention has been paid to the problem of analysing fine scale detail. The initial conditions for the fine-mesh model have generally been determined by interpolation from a coarser mesh hemispheric or global analysis. The reasons for this reluctance to tackle the problem of objective analysis of small scale features are not difficult to understand. Primarily the problem is one of data sparsity. It has long been thought that attempts to analyse on a scale which is smaller than that provided by the observing network would be doomed to failure. The recent introduction of high resolution satellite data from the HERMES system (Turner et. al. 1985) has, however, provided one impetus for the development of a fine-mesh analysis system.

Another difficulty, which has slowed the development of fine-mesh analysis systems in operation numerical weather prediction centres, is the problem of initialisation. Conventional non-linear normal mode initialisation schemes have proved to be rather difficult to apply to limited area models because their solution is complicated by the presence of lateral boundary conditions. Bourke and McGregor (1983) have developed techniques for overcoming these problems, but such complications don't in fact arise with the scheme adopted by the Meteorological Office. The repeated insertion scheme, which was first developed by Lyne et al, (1982) for global data assimilation, has been designed to minimise the excitation of spurious gravity waves. Small observation increments are added to the model fields, which are assumed to be sufficiently in balance, at each timestep, so that the model is not forced too far from a 'balanced state'

and the requirement for any further initialisation is eliminated. It is relatively simple to adopt such a scheme for use with a limited area fine-mesh model.

Apart from the observations, the other component of any analysis scheme is of course the forecast model itself. The detail provided by fine-mesh forecasts is very impressive (Woodroffe, 1984) and although spurious features are occasionally developed, we now have sufficient confidence in the fine-mesh fields to use them as the basic starting point of the analysis in preference to the smoother coarse mesh fields. We would expect to retain the fine-mesh forecast structure in subsequent analyses, especially in data sparse regions. We might also anticipate better quality control of observation which define intense features if those features were captured by the data assimilation cycle. The important detailed structure of frontal regions cannot be determined from observations and can only be analysed using a fine-mesh first guess. By achieving a frontal analysis on a scale which is consistent with the forecast model being used, the 'spin-up' time during which the fields adjust to the scale of the model is much reduced. The elimination of this 'spin-up' period implies that useful rainfall fields may be obtained from the early stages of a forecast and also features which may be developing rapidly in those early stages would not have their development retarded.

The fine-mesh data assimilation scheme also allows the inclusion of a more detailed model orography at the analysis stage. This makes analysis of surface reports which are influenced by orographic effects more meaningful and also the full effects of a more detailed representation of the mountain is felt from the start of the forecast. The alternative way of including a finer mesh orography is to insert it gradually during the

early stages of the forecast which, as well as generating noise, means that the full benefits are lost.

The next section will describe the fine-mesh data assimilation scheme as it has been implemented operationally. Some of the problem areas will be considered and the reasons for designing the scheme in its present form will be explained. The third section will illustrate, by example, how far the hopes and aims discussed in this introduction have been realised.

The fine-mesh data assimilation scheme

The techniques used for the analysis and assimilation of data for limited area fine-mesh modelling are closely allied to those developed for the operational global data assimilation scheme, to the extent that both data assimilation systems share the same core computer code. Details of the coarse-mesh scheme can be found in Bell (1985) and to avoid undue repetition only a brief outline of the basic scheme will be given here. Additional detail will be given, where the fine-mesh scheme differs from the global scheme.

The first point to note is that the fine-mesh data assimilation is not a continuous cycle. The starting point for making a fine-mesh analysis of time T is an interpolated coarse mesh analysis valid at T-12 hours. This uses a simple bi-linear interpolation to the latitude-longitude fine-mesh grid which has twice the resolution of the coarse mesh model and has the same 15 levels and the same terrain following vertical coordinate system. The fine-mesh domain is shown in Fig 1., the grid points marked by the crosses are about 75 km apart in the vicinity of the UK. Lateral boundary values are required to allow for the movement of synoptic features through the edges of the forecast region. The boundary tendencies for the prognostic variables are derived from a coarse mesh forecast starting from

the same coarse mesh analysis at T+12 which was used to provide the interpolated fine-mesh field. These tendencies are applied throughout the data assimilation period as well as the subsequent forecast. Fuller details of the boundary updated scheme are given in Dickinson (1985), which also describes the integration scheme and the physical parametrisations. The necessity for lateral boundary updating is one reason why this intermittent data assimilation cycle has been adopted for the fine-mesh model in preference to a continuous cycle. The boundary updating scheme involves the specification of interpolated coarsemesh values at the fine-mesh boundary points and a continuous assimilation cycle would involve using boundary values from a succession of coarse mesh forecasts. This procedure would introduce a shock to the fine-mesh model whenever the boundary values are introduced from a new coarse mesh forecast since they would be incompatible with previous values. The gravity waves generated would make quality control of observations for the fine-mesh analysis rather difficult since the first guess fields would be contaminated by noise. The intermittent data assimilation cycle also makes the subjective monitoring of the analyses by the forecasters in the Central Forecast Office rather easier because the coarse mesh and fine-mesh solutions cannot diverge too far from one another.

The data assimilation cycle consists of four separate 3 hour assimilation periods as illustrated in Figure 2. The observations used in each period are those which are valid at T-9, T-6, T-3 and T+0 hours respectively. An observation time window of $\pm 1^1/_2$ hours allows all observations which fall within that 3 hour window to be used, with the exception of surface data which is included only if verifying at the analysis time. This contrasts with the coarse mesh data assimilation cycle

which is based on 6 hour assimilation periods each with a 6 hour time window for the observations. Thus, in the fine mesh scheme the asynoptic data, such as aircraft reports and satellite soundings, are used at a time which is closer to the observation time and also the surface observing network can be used at the secondary hours (3z, 9z, 15z, 21z). The adjustment of the model orography to fine-mesh values in the first period (3z or 21z) does however preclude the use of surface pressure information at these stages. This more frequent insertion of data with a smaller time window is likely to be particularly beneficial when the observations are able to identify small scale, rapidly moving features. The fine-mesh analyses also makes use of a more comprehensive surface station network in Europe, where in the coarse mesh only a subset of the network is used for reasons of economy. To avoid unnecessary disturbance near the boundaries of the domain, observations are excluded from a zone near the boundary, where an enhanced diffusion is applied.

A single cycle of the assimilation is illustrated schematically in Figure 3. The quality control, selection and weighting of observations for a fine-mesh analysis uses the same three dimensional univariate optimum interpolation procedure as the coarsemesh analysis, with only a few small modifications.

The first of two complementary quality control checks involves the raising of a flag on every observation which departs substantially from the first guess field which in the fine-mesh scheme is a 3 hour fine-mesh forecast verifying at the observation time.

$$(\psi_{OB} - \psi_{FG})^2 \geq N_1^2 \, (\epsilon_{OB}^2 + \epsilon_{FG}^2) \qquad (2.1)$$

The observation ψ_{OB} is suspect if the inequality in equation (2.1) is satisfied, where ψ_{FG} is the first guess value at the observation point and

ε_{OB}, ε_{FG} are the assumed errors for observation and first guess respectively.

The suspect observations are not allowed to quality control other observations in the second check but they may be reinstated if their departure from the expected analysis using neighbouring observations does not exceed a predetermined level as given by equation (2.2). Conversely observations which satisfy equation 2.2 are rejected.

$$(\psi_{OB} - \psi_{INT})^2 \geq N_2^2 \ (\varepsilon_{OB}^2 + \varepsilon_{INT}^2) \qquad (2.2)$$

The interpolated analysis ψ_{INT} and expected analysis error ε_{INT} are given by equations (2.3) and (2.4) respectively.

$$\psi_{INT} = \psi_{FG} + \Sigma_i \ W_i \ (\psi_{OB} - \psi_{FG})_i \qquad (2.3)$$

$$\varepsilon_{INT}^2 = \varepsilon_{FG}^2 - \Sigma_i \ W_i \ (\varepsilon_k \varepsilon_i)_{FG} \qquad (2.4)$$

The weights W_i are found by solving the set of equations (2.5).

$$(\varepsilon_k \varepsilon_i)_{FG} = \Sigma_j \ W_j \ ((\varepsilon_i \varepsilon_j)_{OB} - (\varepsilon_i \varepsilon_j)_{FG}) \text{ for } i=1,n \qquad (2.5)$$

$(\varepsilon_i \varepsilon_j)_{FG}$ and $(\varepsilon_i \varepsilon_j)_{OB}$ are the first guess and observational error covariances respectively. The summations in equations (2.3)-(2.5) are taken over all selected datum. Ideally all data should be used to interpolate to the analysis point, but for reasons of computationally economy a selection of the best data is made. Best data being defined as those which when taken singly reduce the expected analysis error by the greatest amount.

The optimum interpolation procedure is performed twice. Once to provide an analysis at observation points for the purpose of quality control checks as discussed above, then a second time to select the data and calculate the required weights for determining corrections appropriate to the analysis grid. This optimum interpolation procedure is modified to allow for the higher resolution of the model, in two respects. Firstly the

observation errors are reduced by 10%, from the values used on the coarse-mesh, on the basis that the observations are more representative of an average over the smaller area and hence that component of the error which caters for the unrepresentativeness of the observation may be reduced. This implies a higher weight for the observations. Secondly, a narrower structure function is used as the basis for calculating the first guess error covariance. The width of the gaussian structure function is reduced by a factor $\sqrt{2}$ compared with that used on the coarse mesh. This achieves the aim of analysing small scale features which are identified by the observations.

The next stage of the data assimilation procedure is the assimilation of the interpolation increments as defined by (2.3) directly into the model. This is done during a three hour integration starting at the previous analysis time, using a repeated insertion technique. At each model timestep, a small fraction ($\Delta\psi$) of the weighted average of the difference between the forecast values at that timestep (ψ_M) and the observed values (ψ_i) is added into the model.

$$\Delta\psi = \Sigma \ W_i \ (\psi_i - \psi_M)$$

$$\psi_{n+1} = A(\psi_n) + P(\psi_n) + D(\psi_n) + \lambda_n \ (\Delta\psi_n + G(\Delta\psi_n) + H(\Delta\psi_n)) \qquad (2.6)$$

The assimilation equation is represented by (2.6), where operator A represents the forecast equations, operator P represents the physical parameterisation processes and operator D represents a damping term which is required to suppress gravity waves generated during the assimilation process. These gravity waves generally have a larger divergent wind component than meteorological motions and divergence diffusion which has no effect on the vorticity is used to control them. A damping coefficient of

$2.5 * 10^6$ $m^2 s^{-1}$ is used. The other three terms are all scaled by a relaxation coefficient λ_n which increases linearly with time during the assimilation period. As indicated in Figure 4, at the start of the assimilation period the assimilation increments ($\Delta\psi$) may be large and are therefore given a small weight. As the fields adjust towards a state defined by the observations during the assimilation period the assimilation increments become smaller and a larger relaxation coefficient may be used without generating too much noise. For mass field information the final value of λ is 0.175, but for wind data a smaller value is used during the last few timesteps of the period in order to suppress undesirable surface pressure oscillation at the start of the subsequent forecast. The additional operators G and H represent geostrophically derived wind increments and hydrostatically derived temperature increments respectively. These are designed to hasten the fit of mass field data and are fully described in Bell (1985). Geostrophic wind increments are easier to use in the fine-mesh scheme, because the narrower structure function for the first guess error correlation gives a smoother temperature increment field upon which the geostrophic wind increments are based.

3. Some results of the scheme

a) Direct impact of additional data.

The same basic set of observations are used in any analysis whether coarse-mesh or fine-mesh. Both aim to make best use of all available data. Two components of the observing network do however produce information on a scale which is equivalent to the fine-mesh model grid. These are LASS data, the locally retrieved satellite temperature soundings and the European surface observation network. Figures 5 and 6 give examples of the density of these types of observations. Unfortunately the potential for more

detailed analyses based on the direct impact of such data has yet to be realised. Bell and Hammon (1985) have discussed the problems with LASS data in some depth. Although a lot of detail is evident in the observed thickness fields, it has proved difficult to identify what detail is real and what is spurious. Significant biases have been noted at low levels and near the tropopause, caused by cloud clearing problems and also the use in the retrieval process of a poor climatological first guess. All of these factors contribute to the problem of analysing and adequately assimilating the information from LASS data. Lorenc et. al. (1985) have described methods by which these weaknesses may be overcome.

The problem of extracting fine-scale information from the surface observing network is equally intractable. We are uncertain how representative the reports are of grid box mean fields, particularly where local orographic effects may be large. We are also uncertain how to spread the surface information into the lower troposphere. Ideally one might wish to contain the influence of surface information to the boundary layer, but the required flexibility to do this has not yet been established. At the present time the only use made of surface synoptic reports is the surface pressure information. The indirect impact of the data is more significant. When one considers how the data interacts with the fine-mesh forecast model and the fine-mesh orography the benefits are more obvious as the following sections will show.

b) Impact on analysis of using a more detailed orography

Much fine scale detail at the surface over land is as a result of orographic influences and even if this detail is evident from observations on a 75 km finemesh scale, it is unlikely to be analysed correctly if a coarse orography is used. Fig 7 illustrates the coarse mesh orography for

Western Europe, it being the mean height for a 150 km grid mesh. It is clear that only the largest features are resolved on this scale. The UK is only identifiable by a single high value representing the Scottish Highlands and another representative of North Wales. The Alps are identified as a single high value of 1800 metres in Switzerland and there is no detail at all in France and Germany. In contrast the finer mesh (75 km mean) orography in Fig 8 shows substantially more detail. In particular, the Alps reach up above 2400 metres and four separate high points are clearly resolved, as is the Rhone valley between the Alps and the Massif Central.

The Alps present a considerable barrier to flow from a northerly direction as the example in Fig 9 for data time 9 Feb 1985 clearly shows. The subjective analysis in Fig 9 has ignored many of the smaller features in the observations which have been influenced by orography on a scale much smaller than 75 kms and which are essentially noise as far as the objective analyses are concerned. Even with small features ignored, it is clear that there is a substantial distortion of the flow around the Alps and through the Rhone valley with associated troughing in the region of the Po Valley. Fig 10 shows the objective analysis for the same data time after four cycles of the fine-mesh data assimilation with a coarse mesh representation of the orography. The flow has only been disturbed slightly by the model Alps in this case and pressure is much too high in Northern Italy where the model has been unable to adjust to the observations because of the inappropriate orographic forcing. Fig 11 is similar to Fig 10 but in this case a fine-mesh representation of the orography has been used. We now have a surface pressure field which more closely resembles the subjective

analysis in terms of the flow around the Alpine barrier and the low pressure to the lee of the Alps.

c) Aspects of quality control

Another potential advantage of the fine-mesh data assimilation scheme is the greater detail that may be available in the first guess field which is used for quality controlling the observations. This is especially important at the surface, but may be also valuable near upper jets. An interesting example, illustrating this point is an intense surface low which moved northeastward across Ireland and Scotland on the 18th October 1985. The intensity of this low was not evident until it reached land, where pressure falls in excess of 20 mb in three hours occurred in south west Ireland. The lowest observed pressure was 966 mb at Valentia, but the coarse mesh analysis could only achieve 979 mb as indicated in Figure 12. The centre was nothing more than a trough extending from the main Atlantic low and was too far north. Part of the problem was a poor first guess which caused the rejection of several observations and made the fitting of the remaining observations more difficult. The fine-mesh data assimilation of the same case is illustrated in Figure 13. Although the fine-mesh scheme has been unable to adjust towards the Valentia observation which was still rejected, two other previously rejected Irish observations were accepted and the resulting analysis was 6 mb deeper and the centre was correctly placed further south. At 18z the low had moved to the north of Scotland and central pressure in the fine-mesh forecasts were 963 and 959 mb from coarse mesh and fine mesh analyses respectively, compared with an observed value of 956 mb. The track of the low in the forecast based on the coarse mesh analysis was much too far west of the observed track whereas the forecast and observed tracks in Fig 13 almost coincide and

perhaps more importantly the forecaster could place more credence in this solution because the analysis was better.

d) Impact of a higher resolution assimilation model

In addition to making the assimilation of observations rather easier as the previous example has shown, we would hope that a higher resolution model would provide more detail in data sparse areas. The analysis based on data for 00Z 10th October 1985 highlight this point very clearly. The subjective analyst's chart for that date is given in Figure 14. The main feature of interest is the system in the Atlantic, where surface reports are completely lacking. The analyst has drawn a low of 998 mb at 30W, based on continuity and satellite imagery, with a warm front extending towards Ireland. Figures 15 and 16 show objective analyses for the same data time from the coarse mesh and fine mesh data assimilation systems respectively. The fields of surface pressure, 1000 mb wind, low level thickness and 700 mb vertical velocity are superimposed. The fine-mesh solution is closer to the truth in several respects. It correctly puts the centre of gravity of the system back near 30°W and it has a sharper definition of the frontal structure as indicated by the vertical motion field. The wind vectors match the subjective analysis with regard to the sharp trough which marks the cold front at 30°W, the sudden decrease in strength of southwesterly at 15°W at the surface warm front and also southwesterly flow in the warm sector which is rather too anticyclonic in the coarse mesh analysis. The different characteristics of the two analyses are very obvious in Fig 17 which shows cross sections through the system along a line of latitude. The horizontal wind shear is much greater in the fine-mesh analysis at 28°W near the cold front. At 850 mb the Northerly component of the wind changes from 10 m/s northerly to 20 m/s

southerly across the frontal zone in the fine-mesh analysis, whereas the comparable figures for the coarse mesh analysis are 5 m/s northerly to 15 m/s southerly. There is a much strong thermal constrast in the fine-mesh analysis, as indicated by the pecked contours, especially at low levels. The fine-mesh solution also gives much stronger vertical motions as indicated by the arrows.

The key test to evaluate the analyses is to determine how good are the subsequent forecasts. Figures 18 and 19 show the evolution of two fine-mesh forecasts one starting from an analysis produced by the fine-mesh data assimilation system (Forecast A) and the other starting from an interpolated coarse mesh analysis (Forecast B). Figure 18 shows T+0, T+6 and T+12 surface pressure charts for the two forecasts with that based on the fine-mesh assimilation above the equivalent run based on coarse mesh assimilation. The left most charts correspond with Figures 15 and 16. The centre pair of charts indicate a 6 mb difference in pressure by T+6 and the two forecasts diverge further by T+12 so that Forecast A is 9 mb deeper than forecast B, with a correspondingly more vigorous circulation. This trend continues in the later stages of the forecasts which are shown in Fig 19, with differences in central pressure of 12 mb, 12 mb and 8 mb at T+18, T+24 and T+30 respectively. The speed and track of the forecast low is similarly in the two runs. In fact as regard position both runs verified very well, as indeed did a coarse-mesh forecast from the coarse-mesh analysis. Table 3.1 below shows the depth of the low at 6 hour intervals from three forecasts with the same data time and also for the verifying subjective analysis.

Verifying Time	Coarse-mesh analysis Coarse-mesh Forecast	Coarse-mesh analysis Fine-mesh Forecast (B)	Fine-mesh analysis Fine-mesh Forecast (A)	Subjective analysis
00Z 10 Oct	1000 mb	1000 mb	998 mb	997 mb
06Z 10 Oct	998 mb	998 mb	992 mb	-
12Z 10 Oct	996 mb	994 mb	985 mb	985 mb
18Z 10 Oct	996 mb	991 mb	979 mb	-
00Z 11 Oct	995 mb	998 mb	976 mb	974 mb
06Z 11 Oct	994 mb	988 mb	980 mb	-
12Z 11 Oct	996 mb	990 mb	986 mb	984 mb

Table 3.1

The forecast B does not depart significantly from a coarse-mesh forecast based on the same analysis until T+12. This gives some indication of the timescale for the model fields to adjust from the coarse-mesh solution to the fine-mesh solution. Had the major deepening of this feature taken place later in the forecast period, then the differences between forecasts A and B would have been much less. This case demonstrates that substantial improvements in the detail of a forecast are likely when using a fine-mesh data assimilation system, particularly if significant developments occur in the early stages of the forecast.

4. Concluding Remarks

Hopefully, the discussion in the preceding section has demonstrated the viability of a fine-mesh data assimilation scheme. Observations can be successfully assimilated into a fine-mesh limited area numerical model in order to produce an objective analysis which is appropriate to the scale of the model, and useful improvements in the quality of subsequent forecasts can be achieved. As well as providing the initial conditions for operational fine-mesh forecasts, we now have a tool which is suitable for

investigating the potential of new high resolution data sources such as that generated by the HERMES system.

References

Bell, R.S. 1985 Operational Numerical Weather Prediction System - Documentation Paper No 3 - The Data Assimilation Scheme. Met O 2b, Met Office Bracknell.

Bell, R.S. & Hammon, O. 1985 Impact of data on the HERMES system on the fine mesh data assimilation scheme - a case study. Met O 11 T. Note 199, Met Office, Bracknell.

Bourke, W. & McGregor, J.L. 1983 Nonlinear Normal Mode Initialisation for a limited area model. MWR Vol 111 No. 12.

Dickinson, A. 1985 Operational Numerical Weather Prediction system - Documentation Paper No 4 - The Weather Prediction Model. Met O 2b, Met Office Bracknell.

Lorenc, A., Adams, W. and Eyre J.R. 1985 The Analysis of High Resolution Satellite Data in the Met. Office. Met O 11 T. Note 212, Met Office Bracknell.

Lyne, W.H., Swinbank, R. and Birch, N.T. 1982 A data assimilation experiment and the global circulation during the FGGE special observing periods. Quart. J.R. Met. Soc., 108, 575-594.

Turner, J., Eyre, J.R., Jerrett, D. and McCallum, E. 1985 The HERMES system. Met Mag Vol 114. No 1355.

Woodroffe, A. 1984 Short-Range Weather Forecasting - A current assessment. Weather Vol 39 p.298-310.

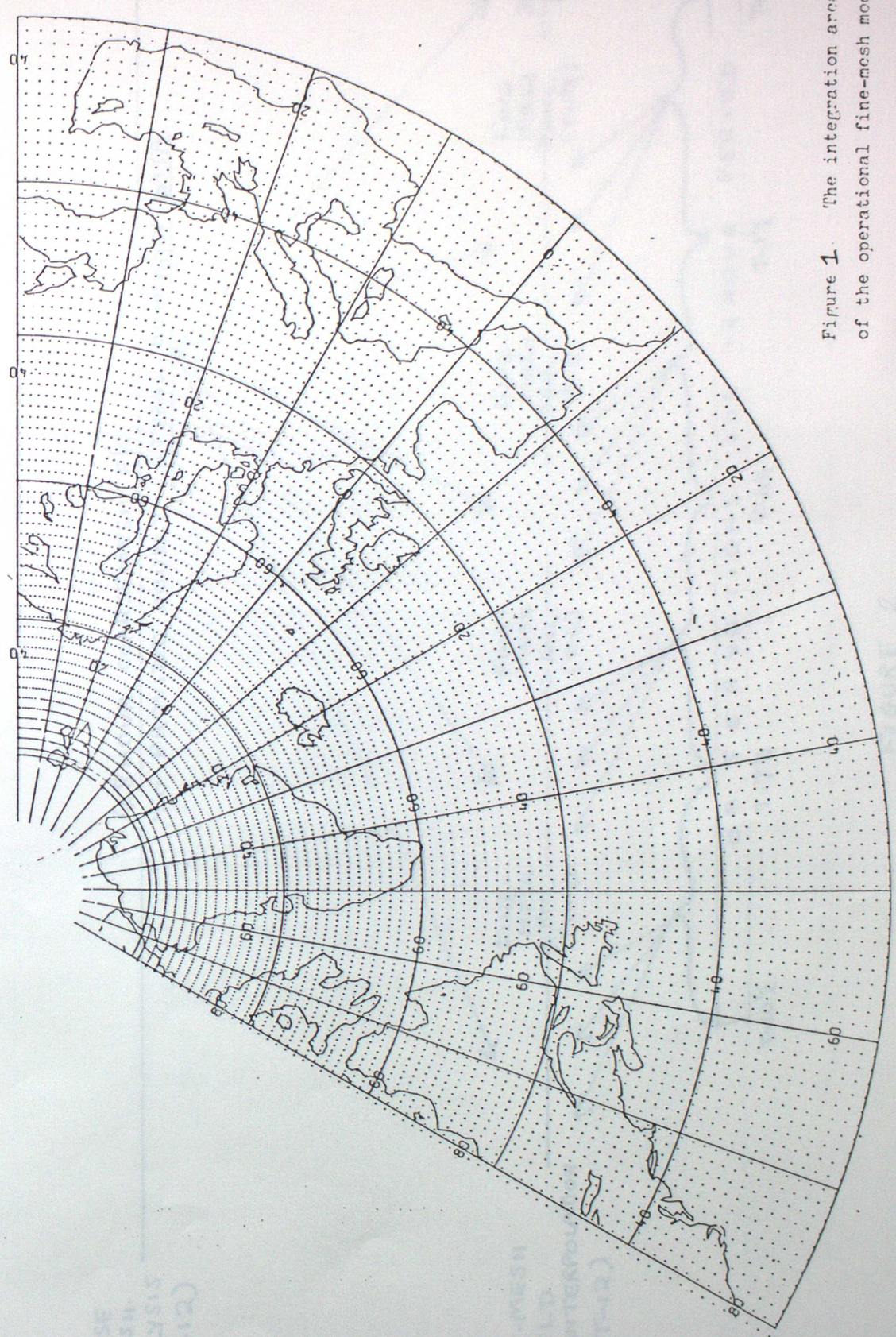

Figure 1 The integration area of the operational fine-mesh model.

OPERATIONAL FINE-MESH DATA ASSIMILATION SCHEME

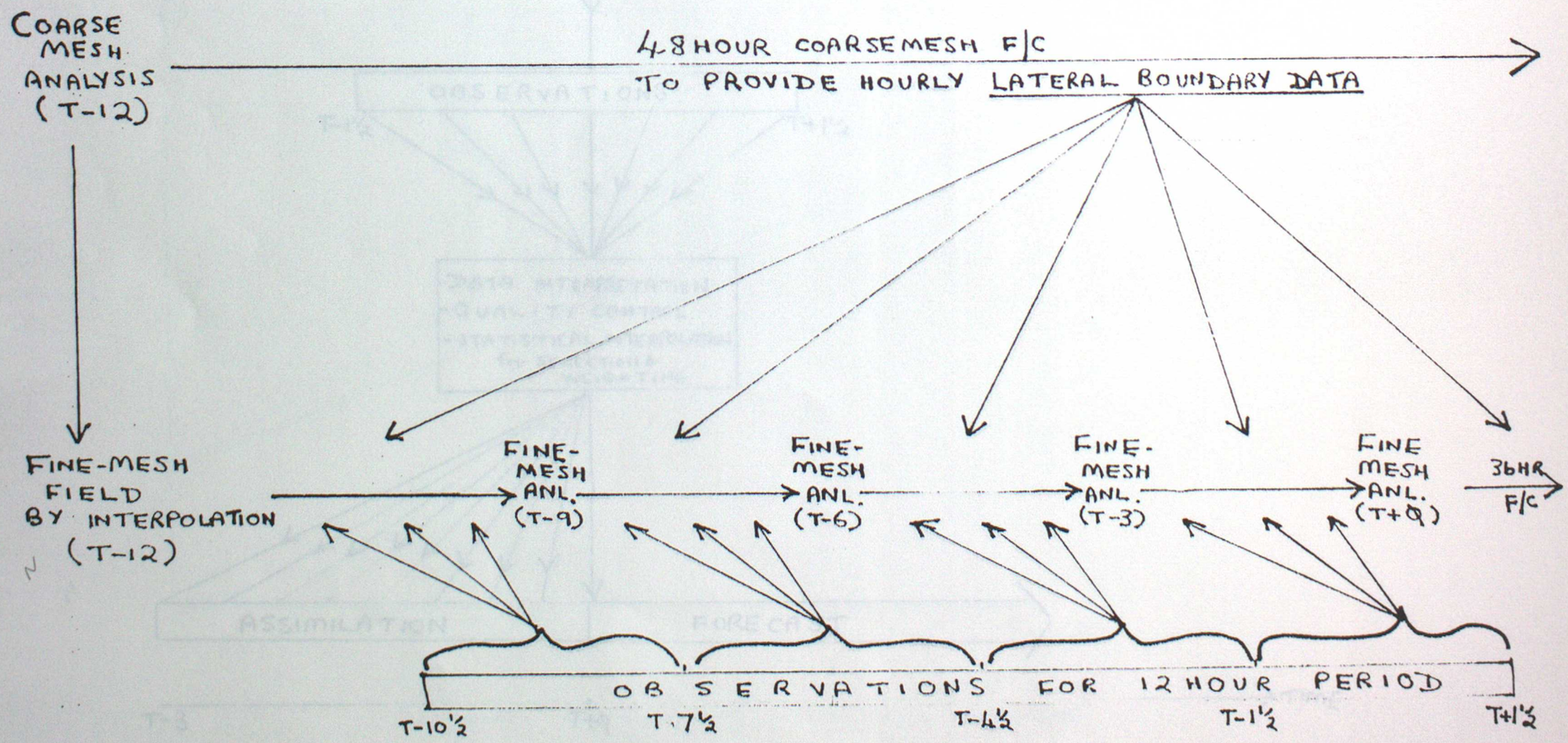

FIGURE 2

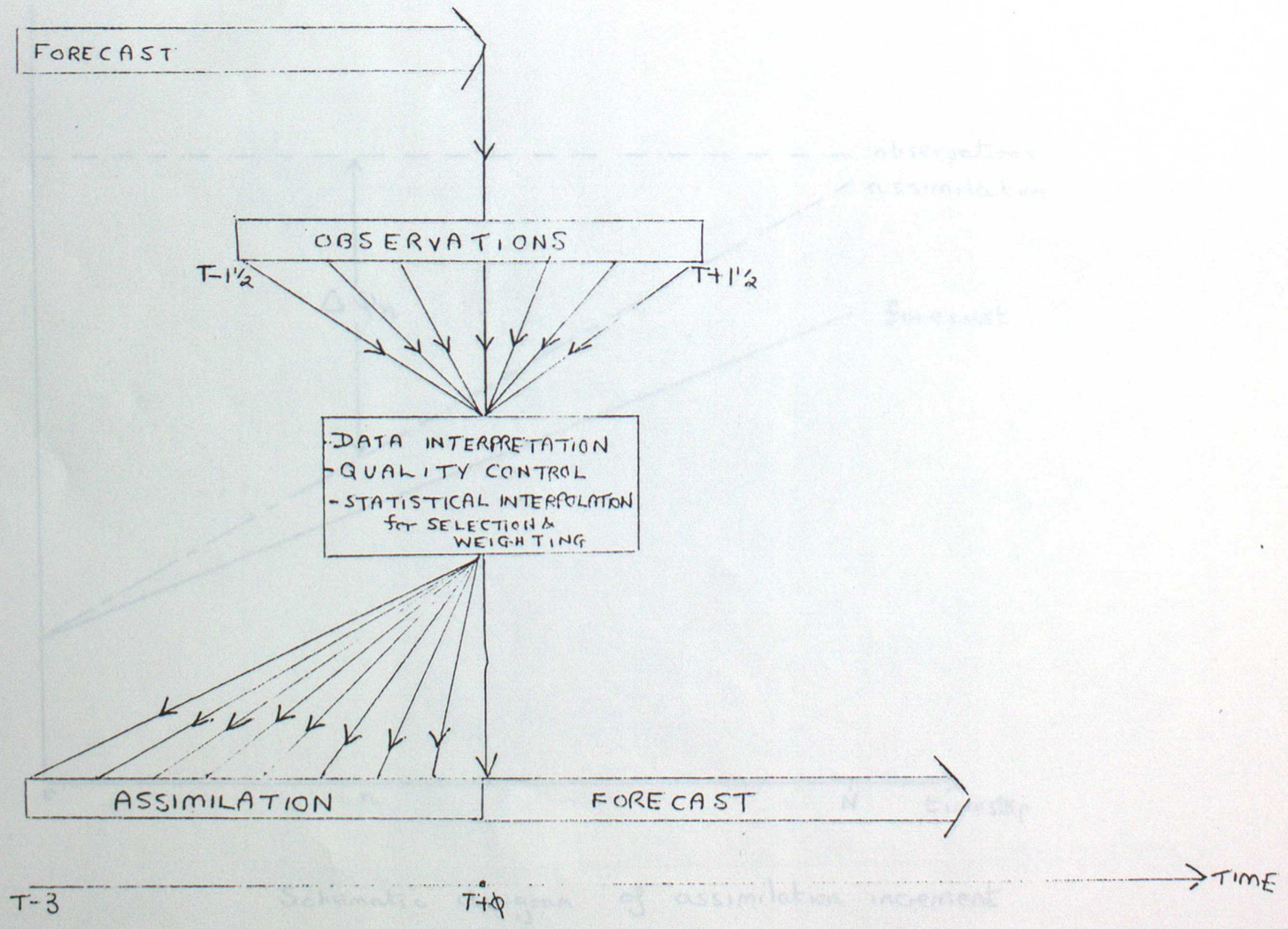

Schematic diagram of assimilation cycle.

FIGURE 3

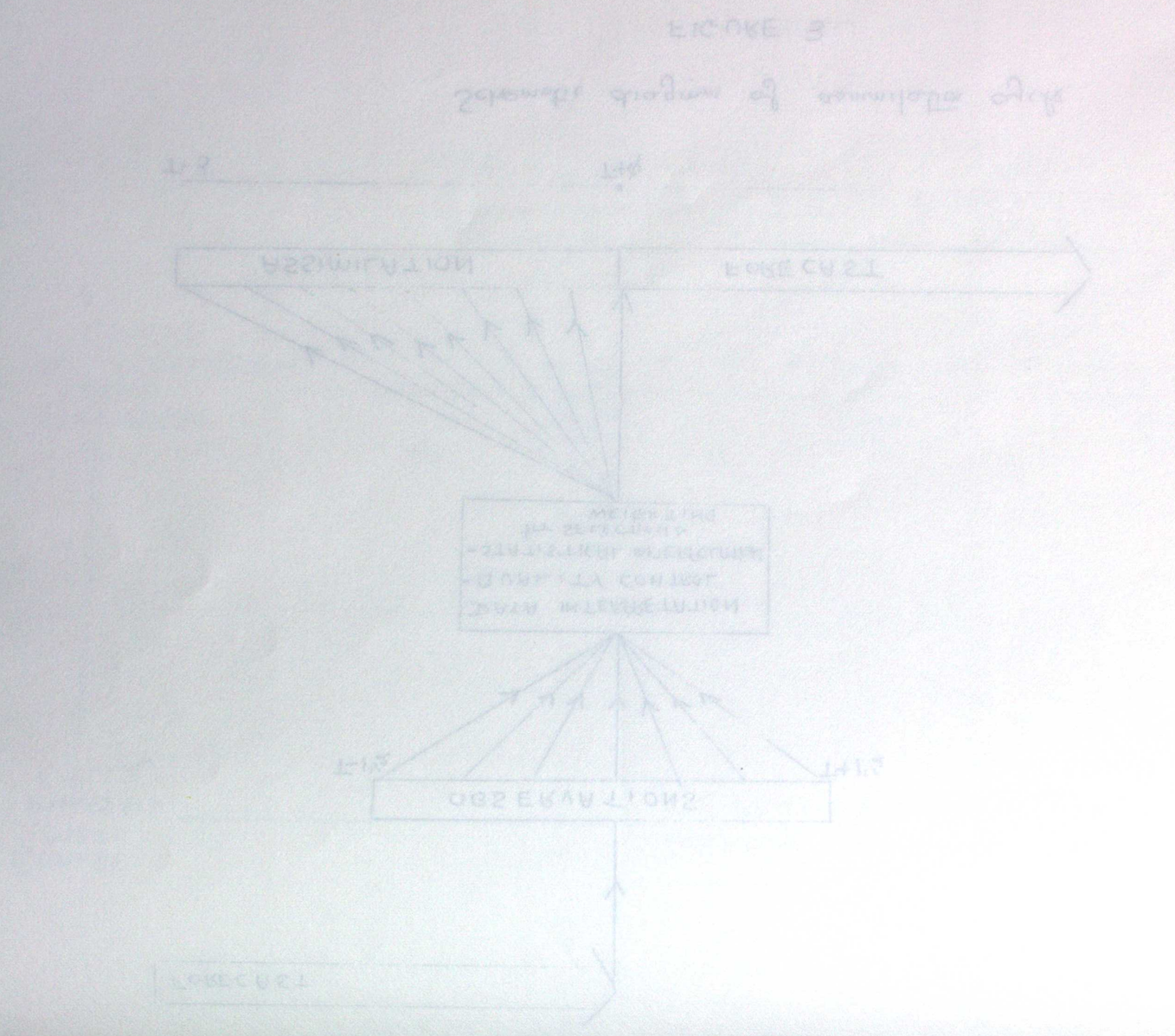

Schematic diagram of assimilation increment

FIGURE 4

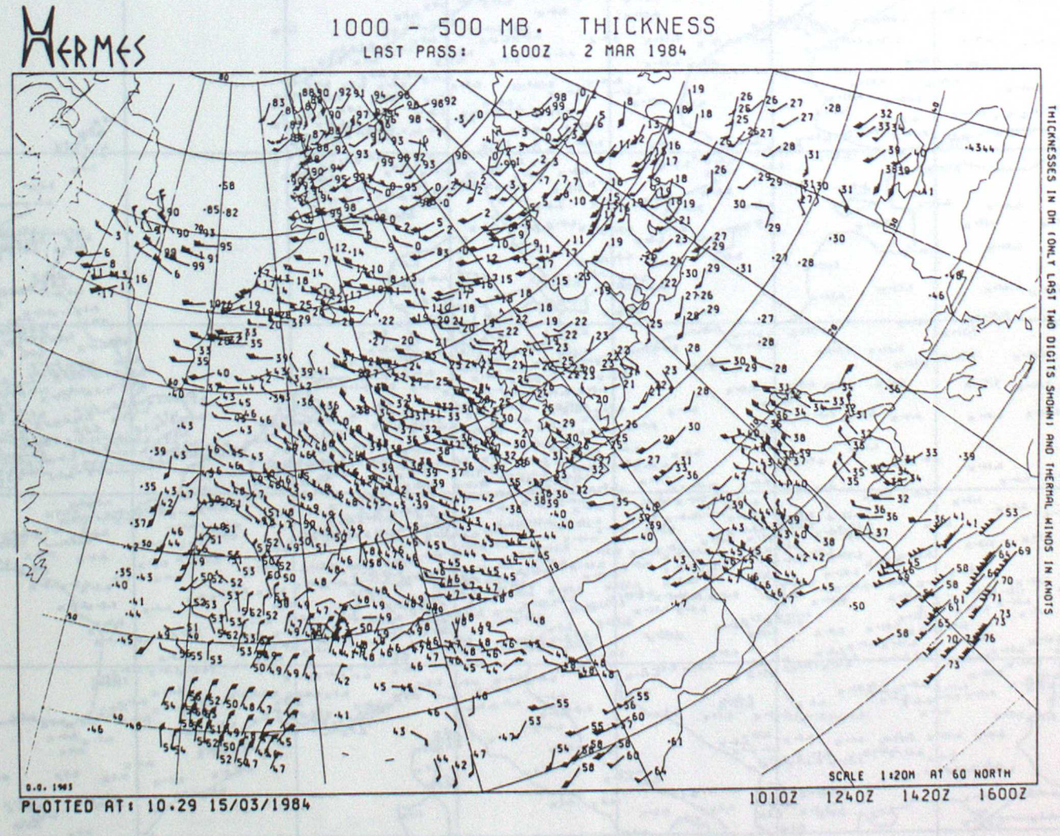
HERMES
1000 - 500 MB. THICKNESS
LAST PASS: 1600Z 2 MAR 1984
THICKNESSES IN DM (ONLY LAST TWO DIGITS SHOWN) AND THERMAL WINDS IN KNOTS
SCALE 1:20M AT 60 NORTH
1010Z 1240Z 1420Z 1600Z
PLOTTED AT: 10.29 15/03/1984

FIG 5


122/12/17/85
25E
20E
15E
10E
5E
0
5W
40N
45N
50N
55N
60N
65N

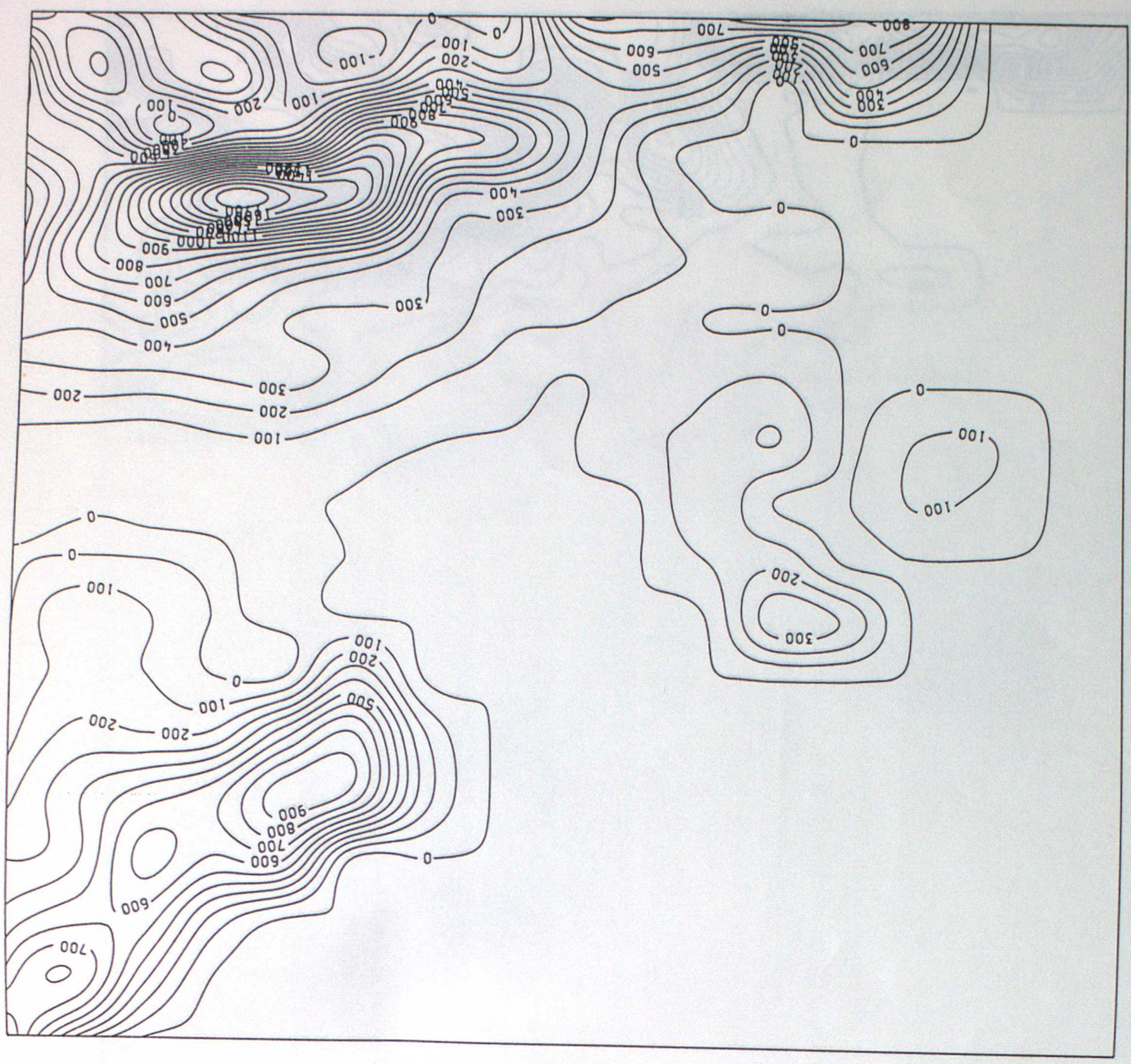

FIG-7

FIG 8

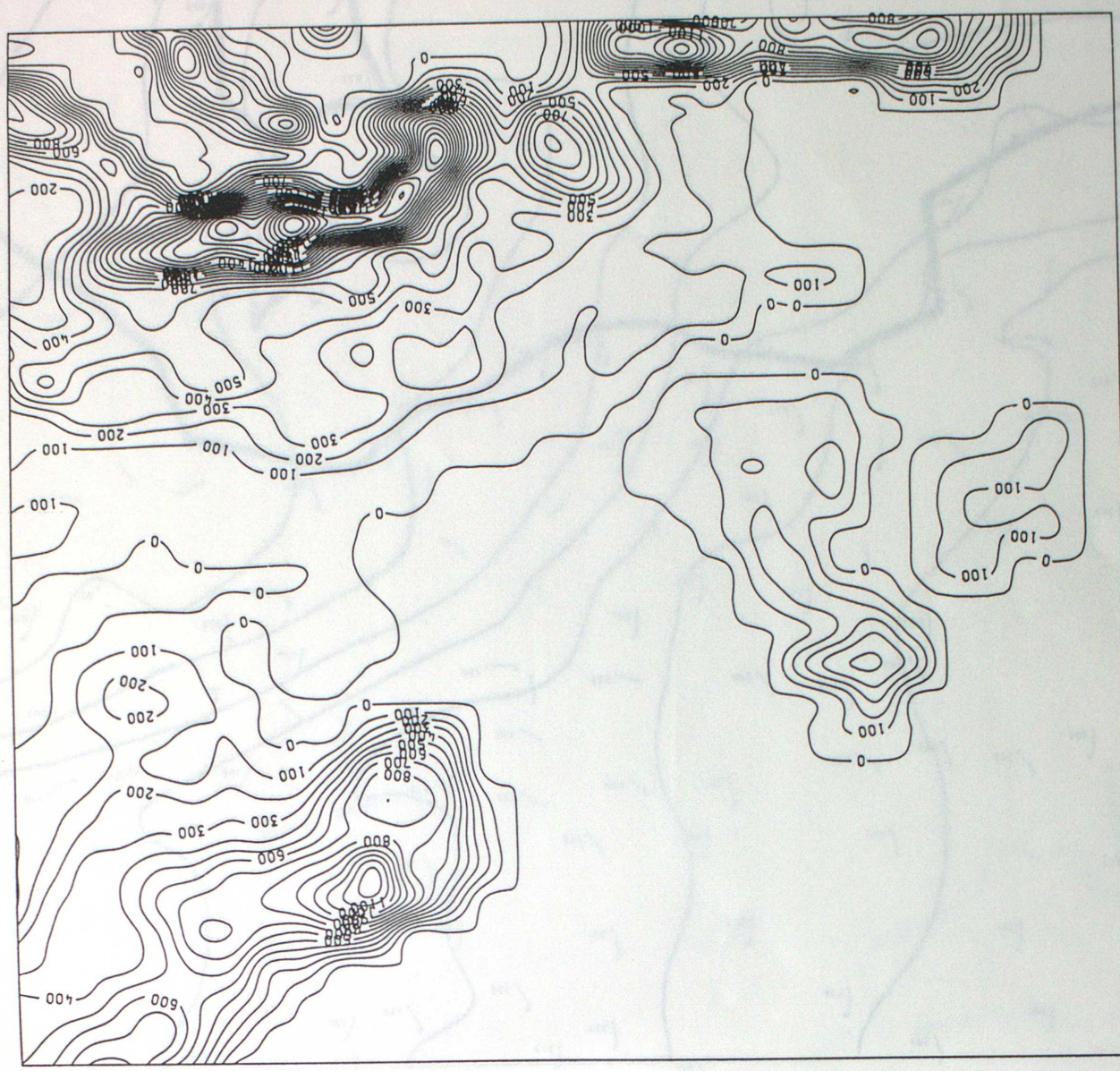

OBSERVATIONS FOR 12Z ON 09/02/1984 LEVEL=SURFACE Fig. 9

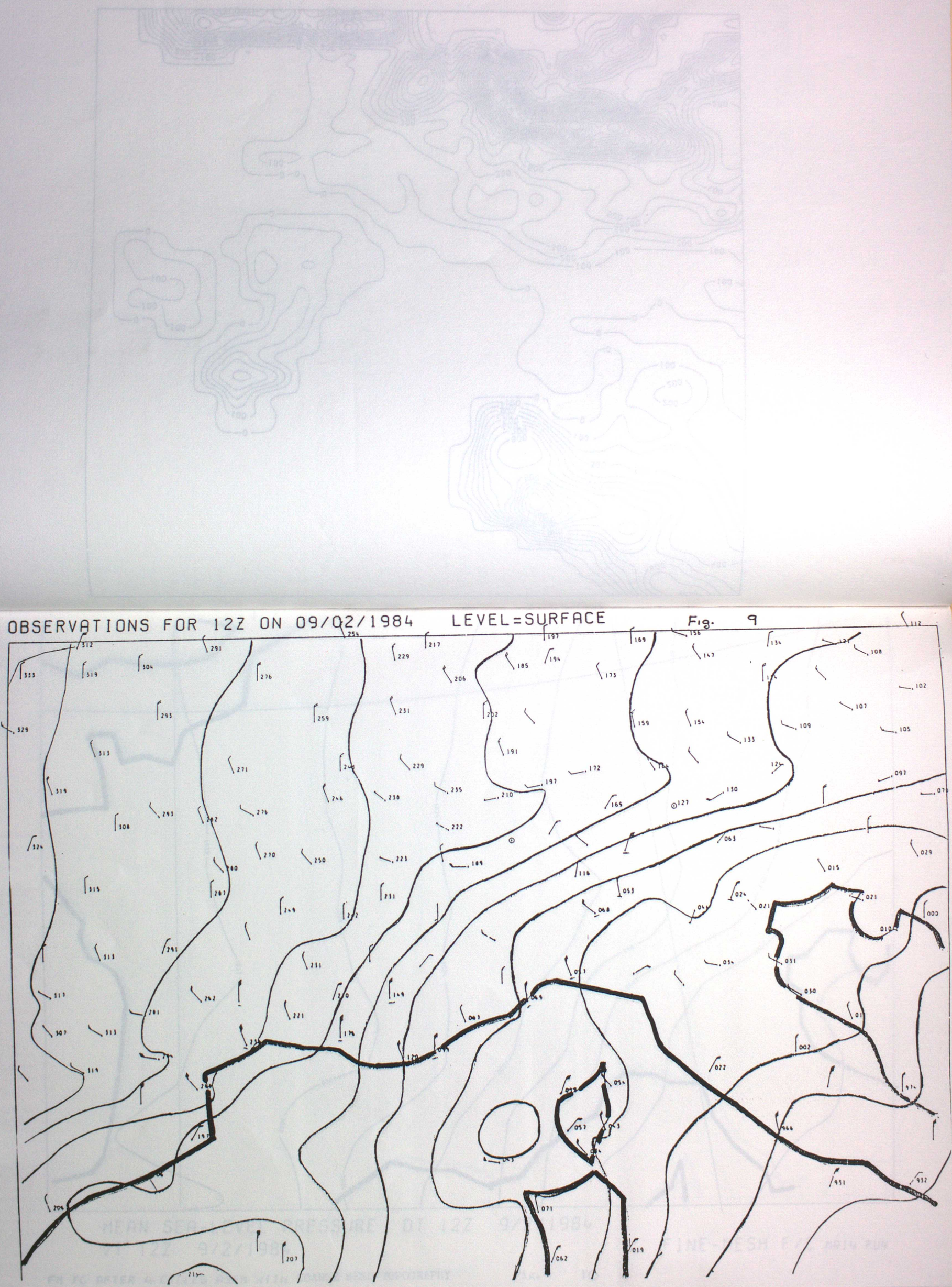

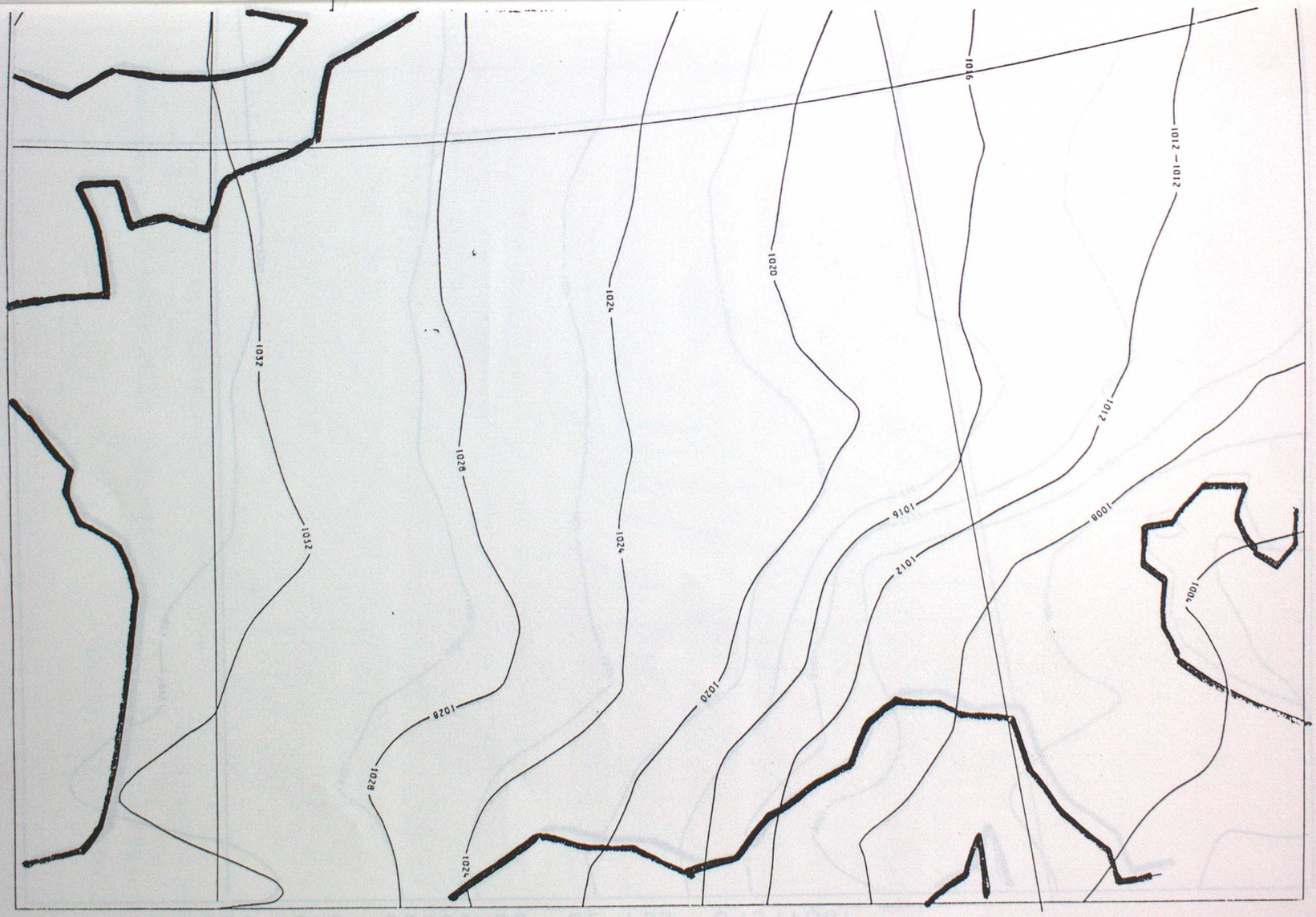

MEAN SEA-LEVEL PRESSURE DT 12Z 9/2/1984
VT 12Z 9/2/1984

FINE-MESH F/C MAIN RUN

FM FC AFTER 4 CYCLES ASSM WITH COARSE MESH TOPOGRAPHY

Fig. 10

MEAN SEA-LEVEL PRESSURE DT 12Z 9/2/1984
VT 12Z 9/2/1984 FINE-MESH F/C MAIN RUN

FMESH FC AFTER 4 CYCLES ASSM WITH FINE MESH TOPOGRAPHY Fig. 11

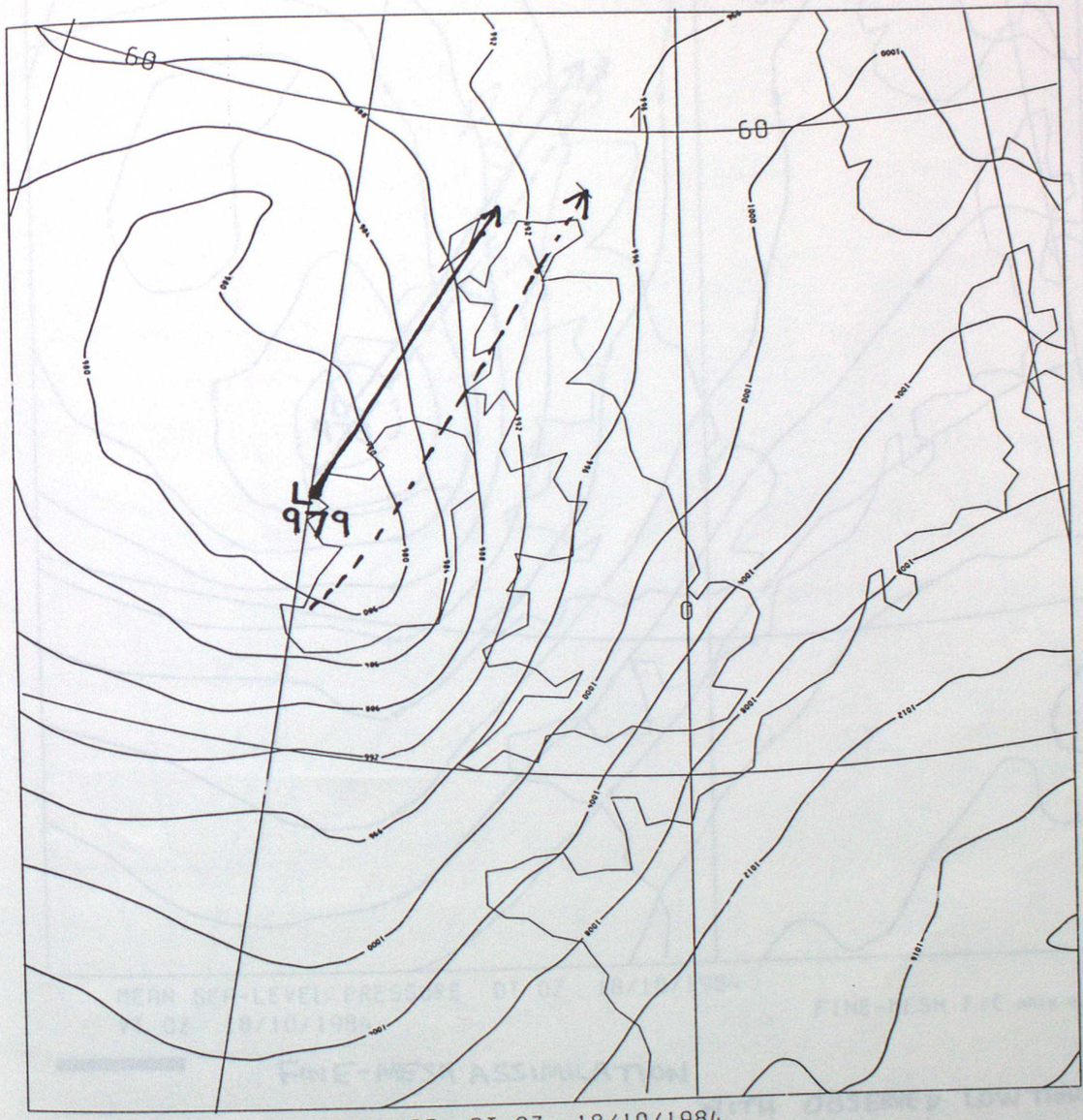

MEAN SEA-LEVEL PRESSURE DT OZ 18/10/1984
VT OZ 18/10/1984

FINE-MESH F/C MAIN RUN

COARSE MESH ASSIMILATION

WITH

OBSERVED LOW TRACK

FORECAST LOW TRACK

Figure 12

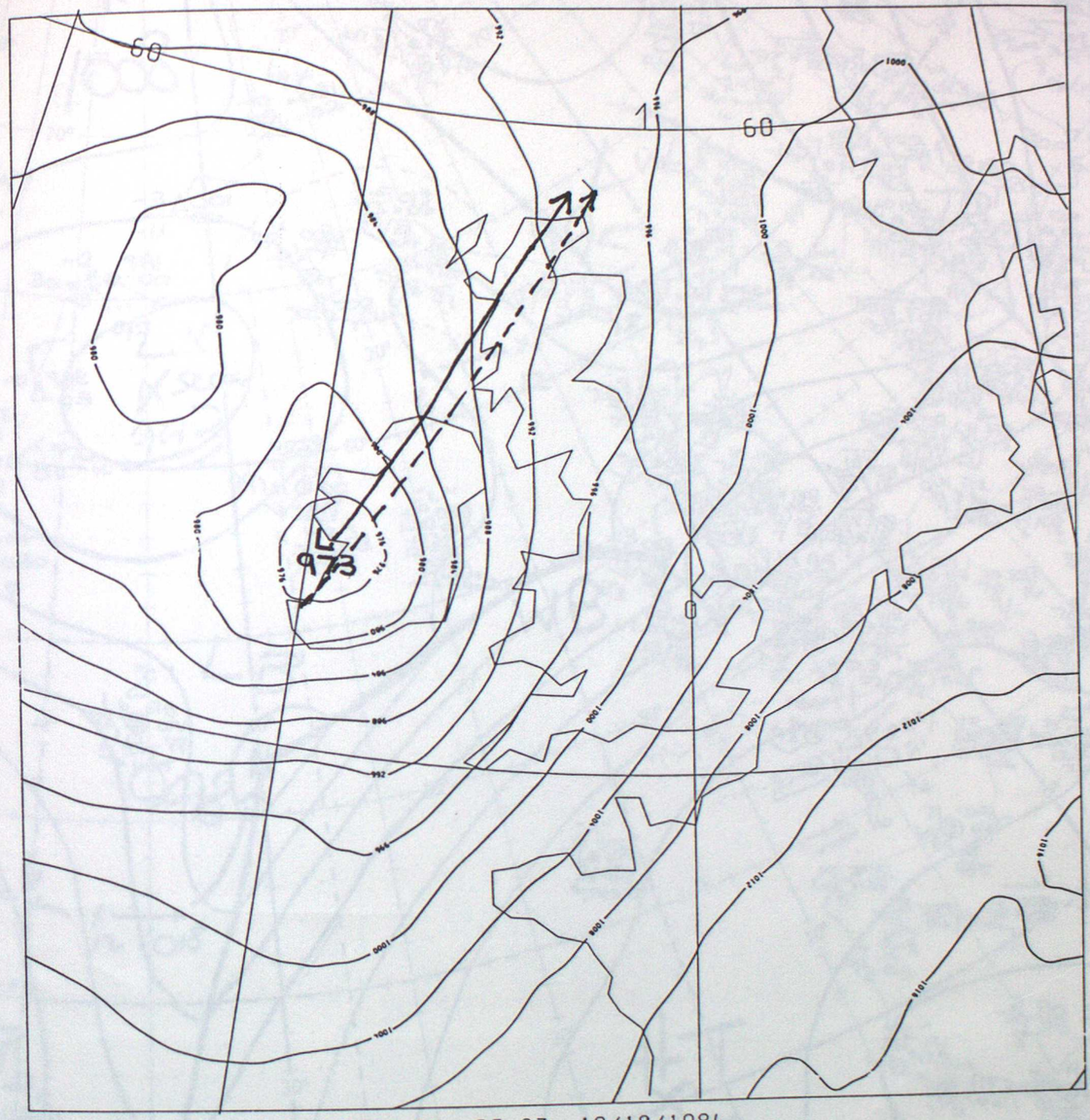

MEAN SEA-LEVEL PRESSURE DT OZ 18/10/1984
VT OZ 18/10/1984

FINE-MESH F/C MAIN RUN

FINE-MESH ASSIMILATION

WITH OBSERVED LOW TRACK

FORECAST LOW TRACK

Figure 13

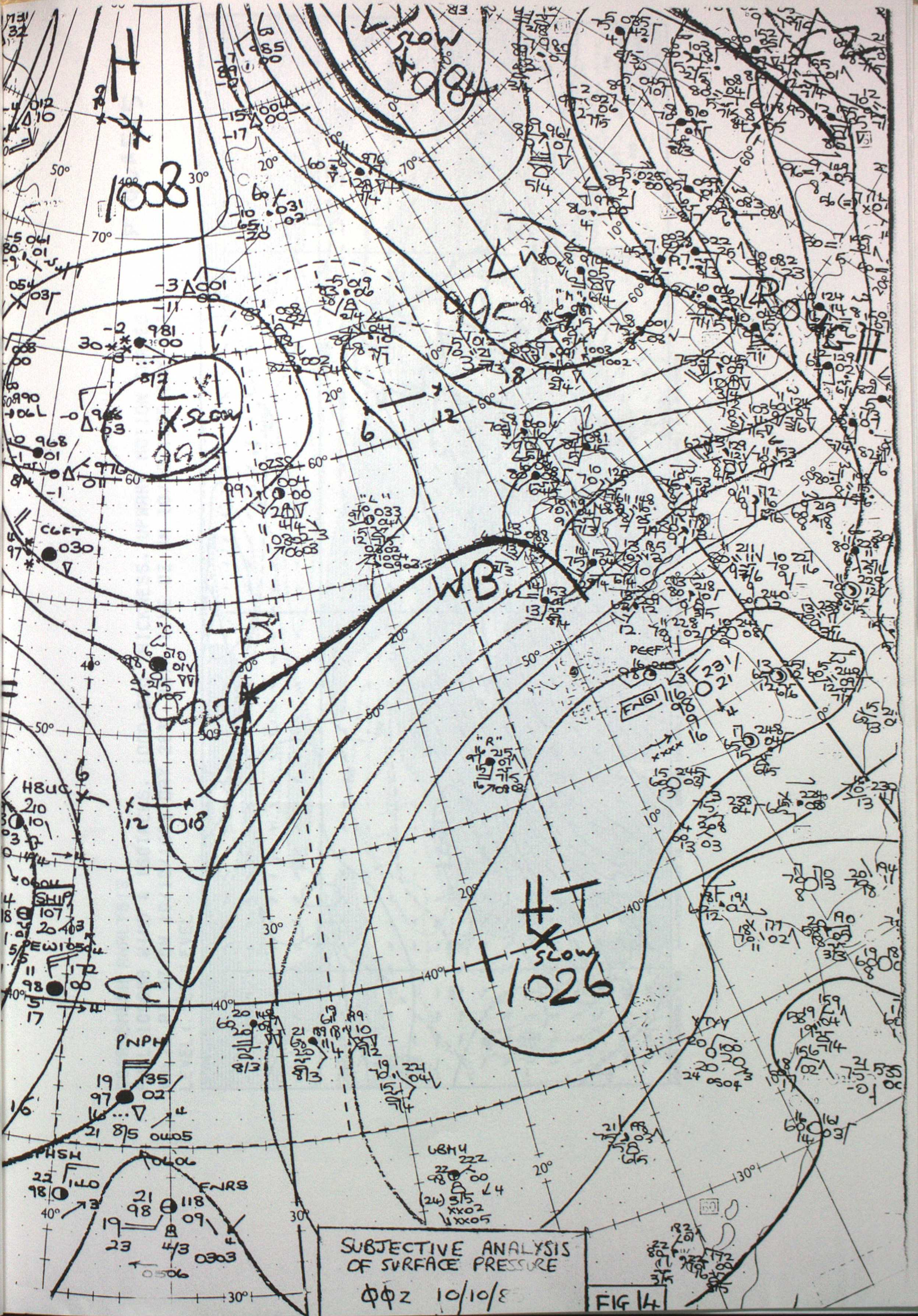

SUBJECTIVE ANALYSIS OF SURFACE PRESSURE ΦΦZ 10/10/8

FIG 14

COARSEMESH ANALYSIS
PMSL,1000MB WIND & ISOTACHS, 1000-850 THICKNESS, UPWARD MOTION SHADED
VALID AT 0Z ON 10/10/1985 DAY 283 DATA TIME 0Z ON 10/10/1985 DAY 283
LEVEL: SEA LEVEL

FIGURE 15

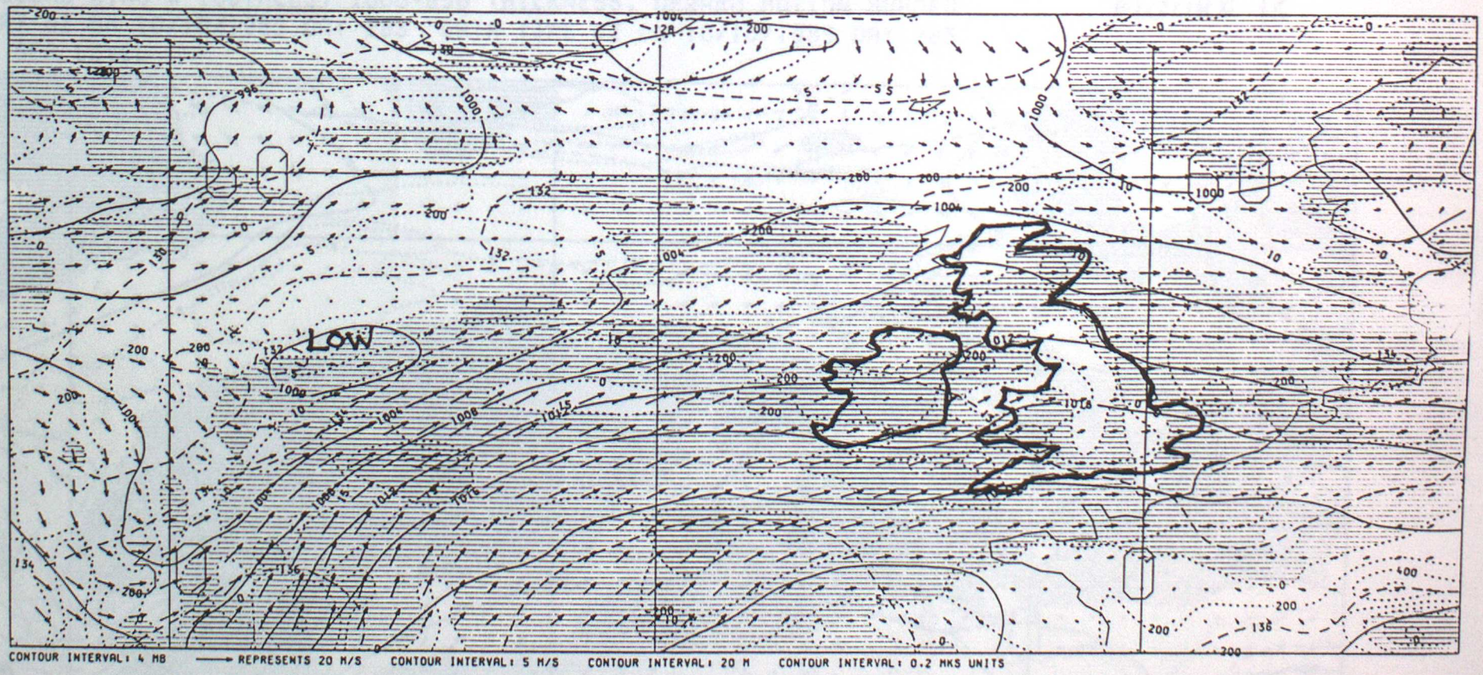

FINEMESH ANALYSIS
PMSL.1000MB WIND & ISOTACHS. 1000-850 THICKNESS. UPWARD MOTION SHADED
VALID AT 0Z ON 10/10/1985 DAY 283 DATA TIME 0Z ON 10/10/1985 DAY 283
LEVEL: SEA LEVEL

FIGURE 16

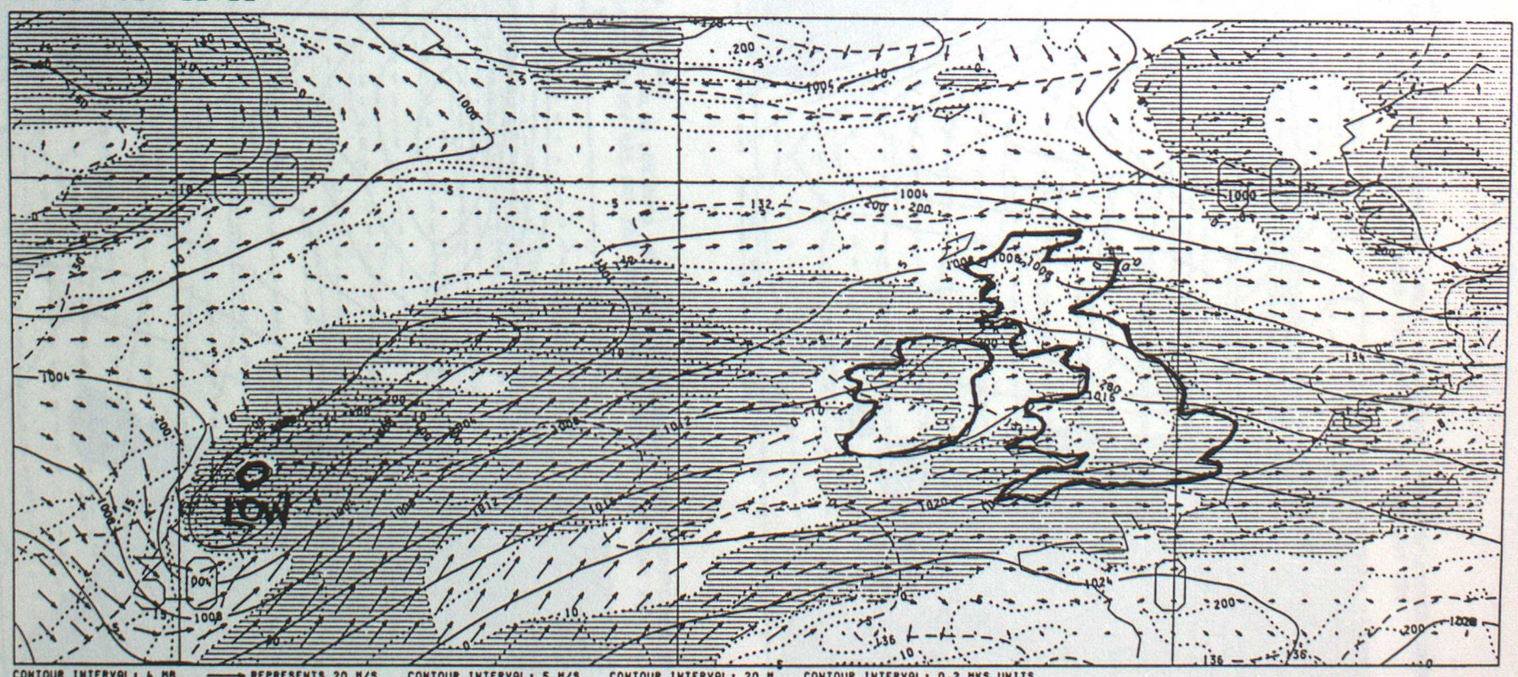

FINEMESH ANALYSIS
E-W X-SECTION. V=SOLID CONTOURS -VE SHADED. U&W=ARROWS. POT.TEMP=PECKED CONTOURS
VALID AT 0Z ON 10/10/1985 DAY 283 DATA TIME 0Z ON 10/10/1985 DAY 283
LATITUDE: 52

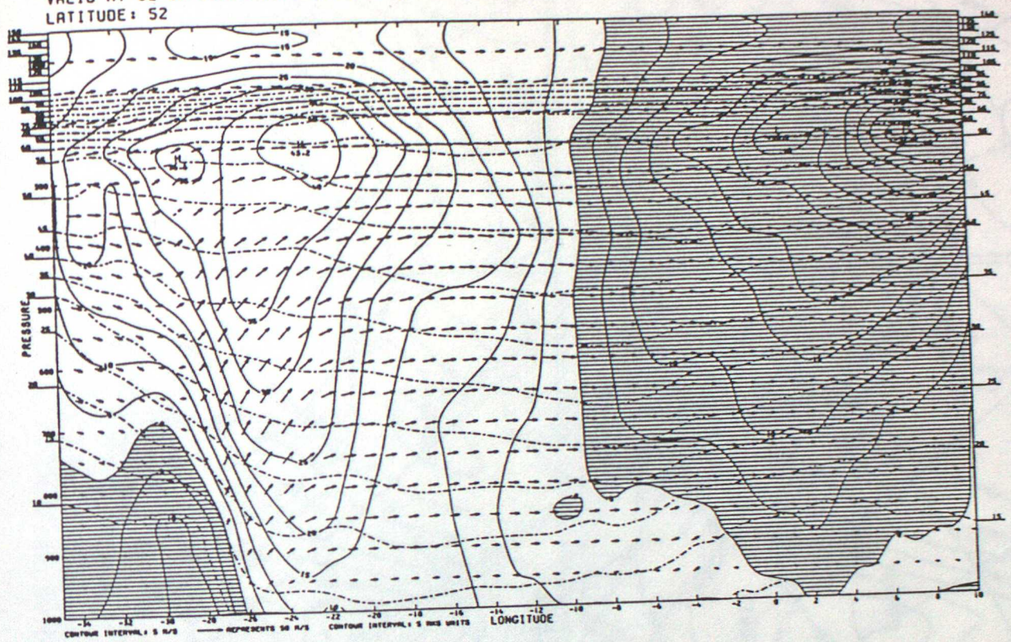

COARSEMESH ANALYSIS
E-W X-SECTION. V=SOLID CONTOURS -VE SHADED. U&W=ARROWS. POT.TEMP=PECKED CONTOURS
VALID AT 0Z ON 10/10/1985 DAY 283 DATA TIME 0Z ON 10/10/1985 DAY 283
LATITUDE: 52

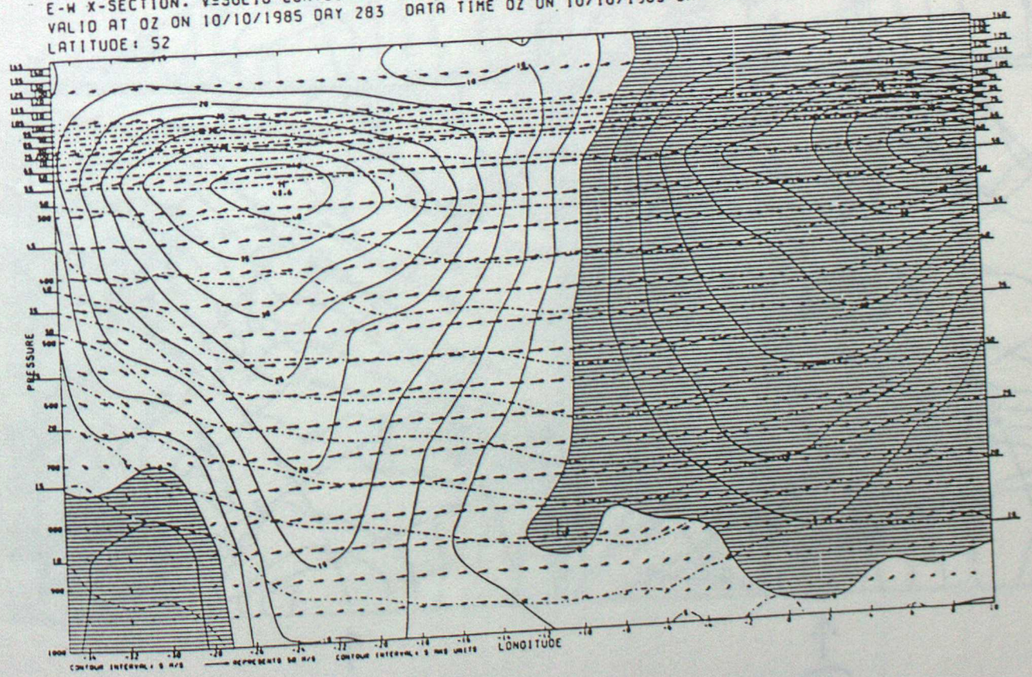

FIGURE 17

FIGURE 18 FINEMESH FORECASTS
from a) finemesh analysis
b) interpolated coarsemesh analysis.

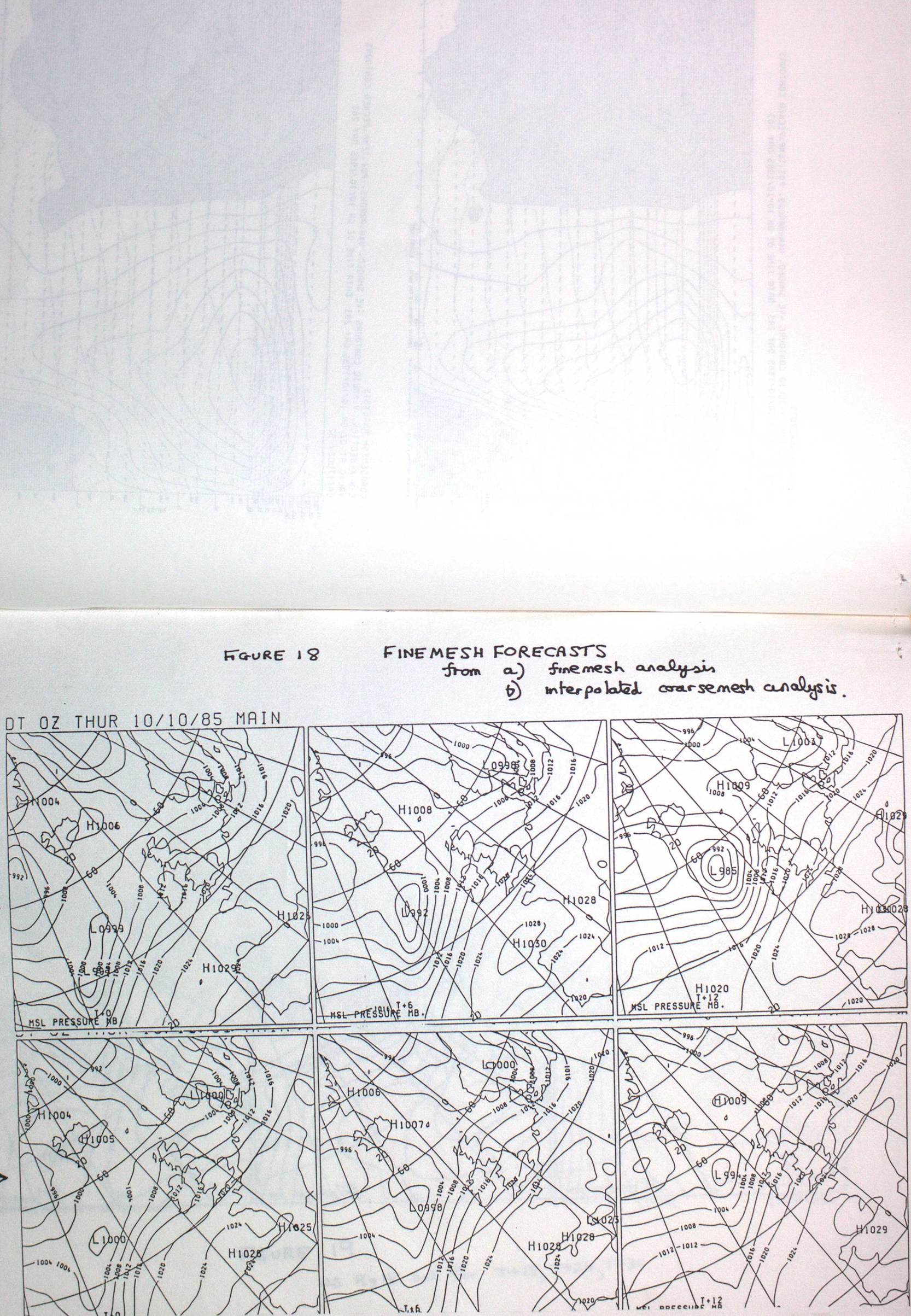

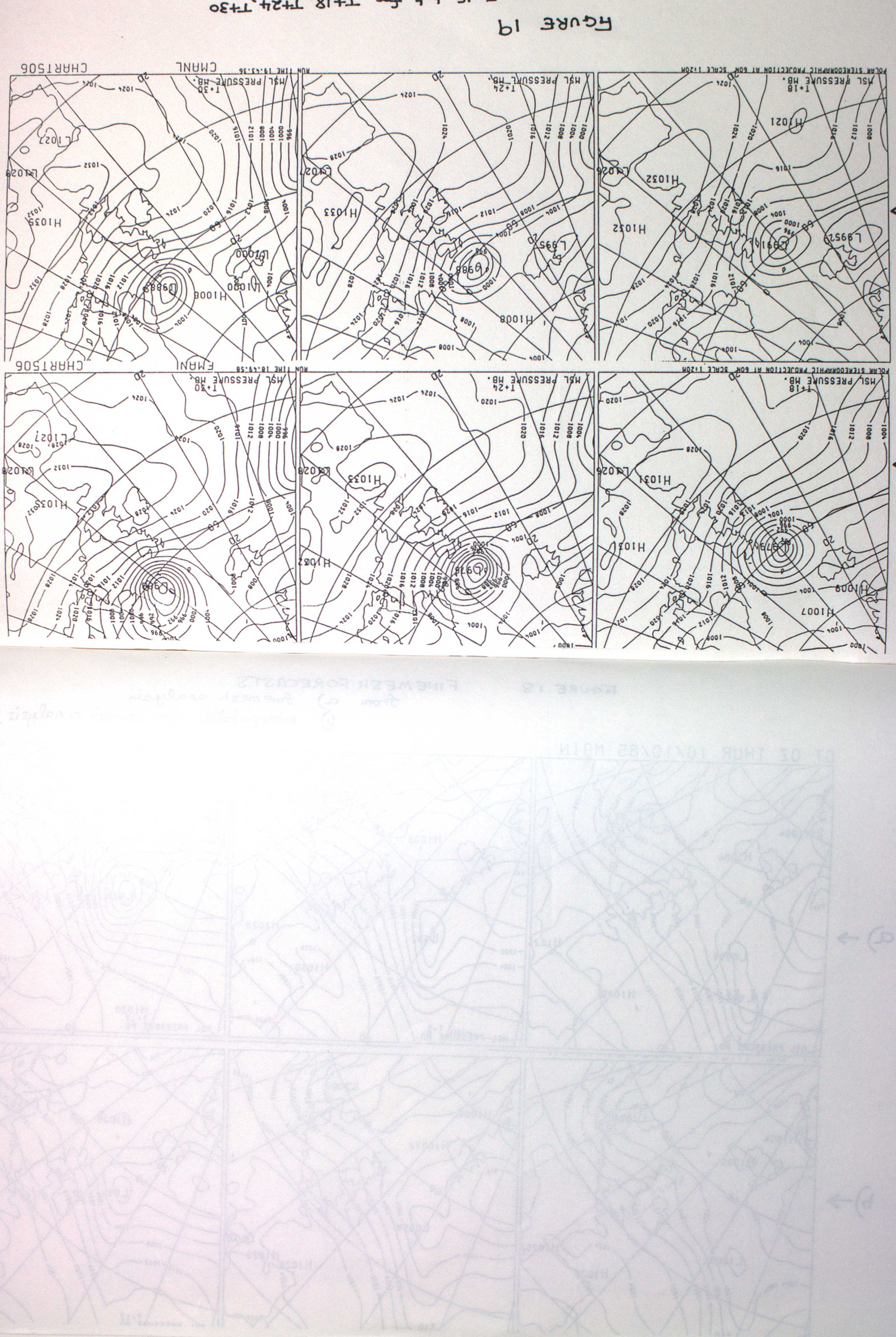

FIGURE 19

as Fig 18 but for T+18, T+24, T+30